American Mineralogist, Volume 96, pages 1575–1584, 2011

Coarsening kinetics of coexisting peristerite and film microperthite over 10^4 to 10^5 years

Ian Parsons[1,*] and John D. Fitz Gerald[2]

[1]Grant Institute of Earth Science, University of Edinburgh, King's Buildings, West Mains Road, Edinburgh EH9 3JW, U.K.
[2]Research School of Earth Sciences, Australian National University, Canberra ACT 0200, Australia

Abstract

Alkali feldspar crystals from the Klokken syenite pluton (South Greenland) have a coarse patch perthite exsolution texture, on the scale of hundreds of micrometers, produced by dissolution-reprecipitation reactions at ~500 °C. We have discovered that Ab-rich patches ($Ab_{92}An_7Or_1$) subsequently exsolved by spinodal decomposition to give peristerite, with a periodicity of 17 nm. This is the first time a peristerite has been characterized by TEM within a perthite, and the first peristerite to be found outside regional metamorphic rocks and pegmatites. The coexisting Or-rich patches, $Ab_{16}Or_{84}$ ($An_{0.3}$), unmixed over the same temperature interval to yield coherent film microperthite with periodicities ≤1 μm. Because the peristerite and film perthite from a single hand specimen from the Klokken intrusion have shared exactly the same cooling history, they provide a novel opportunity to test the utility of diffusion coefficients obtained in the laboratory for prediction of coarsening rates over 10^5 yr time scales, in the light of a calculated cooling trajectory for the pluton. We find good agreement between observed and predicted periodicities for the film perthite, which began to exsolve by coherent nucleation at the coherent solvus for ordered feldspars at ~420 °C, ~32 000 yr after crystal growth, and took a further 13 000–39 000 yr to coarsen to a periodicity of 1 μm. Peristerite exsolution began at the conditional spinodal at ~450 °C, but on the basis of the best existing experimental data would have taken ~520 000–4 600 000 yr to coarsen, incompatible with the cooling history. We speculate on changes to these "best" parameter values to describe NaSi-CaAl interdiffusion that would lead to peristerite coarsening rates compatible with the cooling history of the Klokken intrusion. We find that an interdiffusion expression:

$$D_{\text{NaSi-CaAl}} = (9 \times 10^{-12})\exp(-220\,000/RT)$$

(where D and the pre-exponential term, A, are in units of m^2/s and the activation energy, E_a, is in J/mol) leads to coarsening rates compatible with the experimental data, the cooling path of the Klokken intrusion, and the coarsening rate of the coexisting film perthite. The new interdiffusion parameters are consistent with fine-scale peristerite intergrowths in low-grade metamorphic rocks and with the existence of the coarsest known peristerite. In the light of our discovery, it seems likely that peristerite is commonplace in albitic plagioclase in granitic rocks.

Keywords: Peristerite, perthite, diffusion, kinetics, alkali feldspar, Klokken intrusion

Introduction

We have discovered film microperthite and peristerite intergrowths in Or- and Ab-rich subgrains coexisting within single patch perthite alkali feldspar crystals in the Klokken intrusion (Figs. 1–3). This is the first time a peristerite in the Ab-rich phase of a perthite has been characterized using transmission electron microscopy (TEM), and the first example of peristerite outside regional metamorphic rocks and pegmatites. A cooling history for the Klokken intrusion, calculated by Brown and Parsons (1984b), using the heat diffusion equations of Jaeger (1968), showed that the feldspars would have passed through the temperature (T) interval for exsolution 10^4–10^5 yr after crystallization (Fig. 4). Because the coexisting microtextures have shared exactly the same cooling history, they provide a novel opportunity to assess the use of interdiffusion coefficients for both types of exsolution, determined experimentally over time scales (t) of ≤1.5 yr, to predict lamellar periodicities (λ) over 10^5 yr time scales.

The film microperthite lamellae coarsened relatively rapidly, to ~1 μm, because the process essentially involves only Na-K interdiffusion. The peristerite intergrowths reached λ of only 17 nm during the same T-t history because of the requirement for coupled NaSi-CaAl interdiffusion. We find that for film perthite intergrowths, Na-K interdiffusion coefficients determined experimentally by Yund and Davidson (1978), give lamellar periodicities in excellent agreement with those observed. For the persiterite intergrowths, the NaSi-CaAl interdiffusion coefficients obtained by Liu and Yund (1992), suggest that longer time scales would be required than are implied by the calculated cooling history. However, we are able to suggest changes to the pre-exponential factor (A) and activation energy (E_a) for NaSi-CaAl interdiffusion that are compatible with both Liu and Yund's (1992) experiments and the cooling history of the pluton.

* E-mail: Ian.Parsons@ed.ac.uk

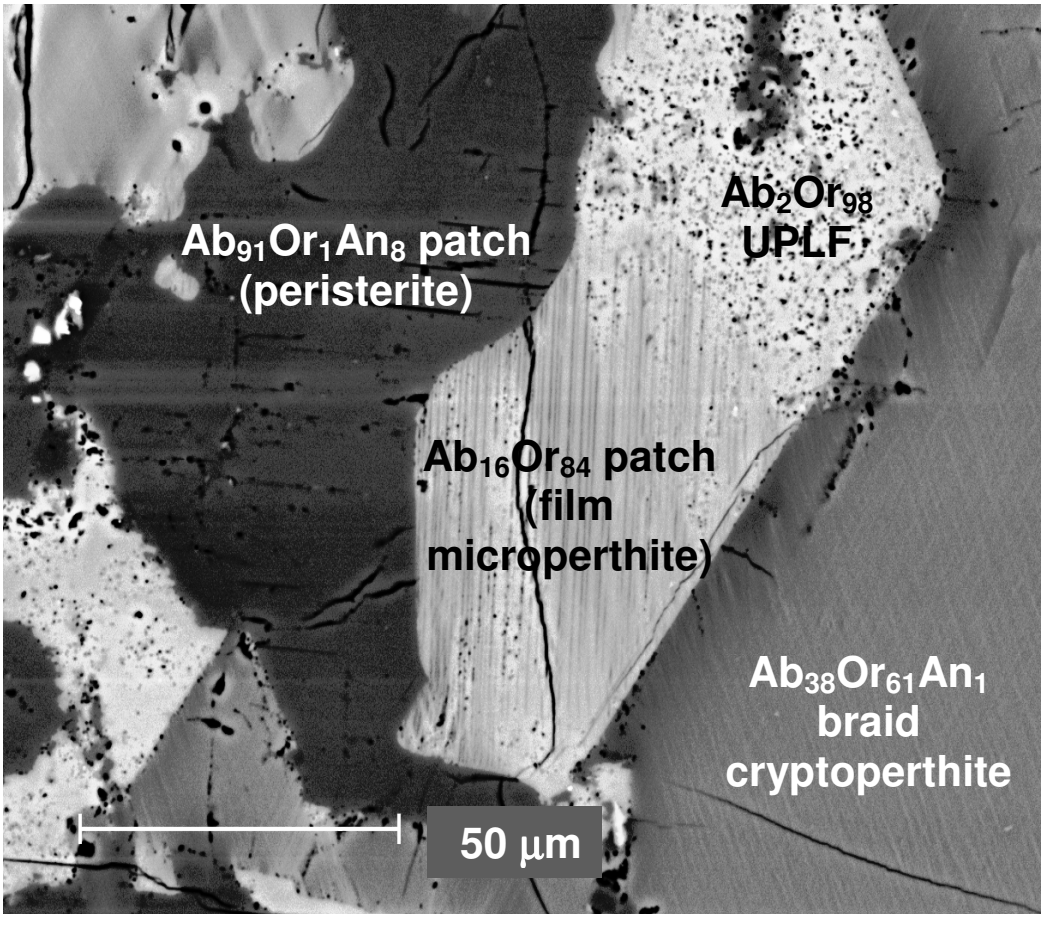

FIGURE 1. Backscattered electron (BSE) image of a polished surface summarizing the relationship of the coherent and the incoherent microtextures within an alkali feldspar crystal in sample KS 41, viewed from approximately normal to (001). Dark areas are Ab-rich, bright areas Or-rich. The bulk compositions of each region are given, obtained by electron microprobe using a large-diameter beam. The braid perthite has a mean λ of ~135 nm (Parsons et al. in prep) and the coarsest lamellae are just visible at this magnification. The Or- and Ab-rich patches are incoherent subgrains formed by dissolution and reprecipitation of the braid perthite. The straight boundaries at the right of center between braid cryptoperthite and a large Or-rich subgrain are in {110}, the low-*T* adularia habit. The Or-rich subgrain subsequently underwent coherent exsolution to yield film microperthite, with λ ~0.5–1 μm. Ab-rich subgrains exsolved to a peristerite with λ ~17 nm, which is therefore not visible at this magnification. UPLF (Ultra Porous Late Feldspar) in this image is mostly near-end-member Or-rich feldspar that has replaced film perthite. The numerous black dots are micropores. The darkest regions of albite in the area labeled UPLF are the equivalent late Ab-rich phase. There are at least eight feldspar phases in this image: low albite and low microcline in the braid intergrowth; low albite and orthoclase in the film intergrowth; albite and oligoclase in the persiterite; near end-member low albite and microcline (adularia) in UPLF.

A detailed account of the crystallography, chemistry, and geothermometry of the film and peristerite intergrowths, and of the very porous, near-end-member feldspars that replace them (Ultra Porous Late Feldspar, UPLF, Fig. 1) will be presented elsewhere (Parsons et al. in prep). Here we concentrate on the coarsening kinetics of the film and peristerite intergrowths. We use the usual abbreviations Ab, Or, and An for the feldspar *components* $NaAlSi_3O_8$, $KAlSi_3O_8$ and $CaAl_2Si_2O_8$, respectively. Although a perthitic feldspar would normally be an intergrowth of two ternary feldspar *phases*, the complex crystals in the present study contain at least eight phases (Fig. 1). All are strictly ternary although the concentration of the An component in the Or-rich phases, and of the Or component in the Ab-rich phases, is sometimes <1 mol%.

BACKGROUND

The Klokken intrusion in South Greenland is a small stock with a layered syenite core (for full details see Parsons 1979). The intrusion has had a remarkably simple thermal history since its emplacement at 1166 Ma (Harper 1988), as demonstrated by $^{40}Ar/^{39}Ar$ work (Parsons et al. 1988; Burgess et al. 1992). Burgess et al. (1992) calculated that it was maintained at a mean ~120 °C since 1166 Ma and never experienced any short-lived event above ~240 °C. The Klokken intrusion is likely to have been emplaced beneath a maximum cover thickness of 3 km (Parsons 1981) and the geothermal gradient may initially have been high. Later intrusions (which are separated from the Klokken intrusion by ~1.3 km and more) apparently did not significantly heat the Klokken body.

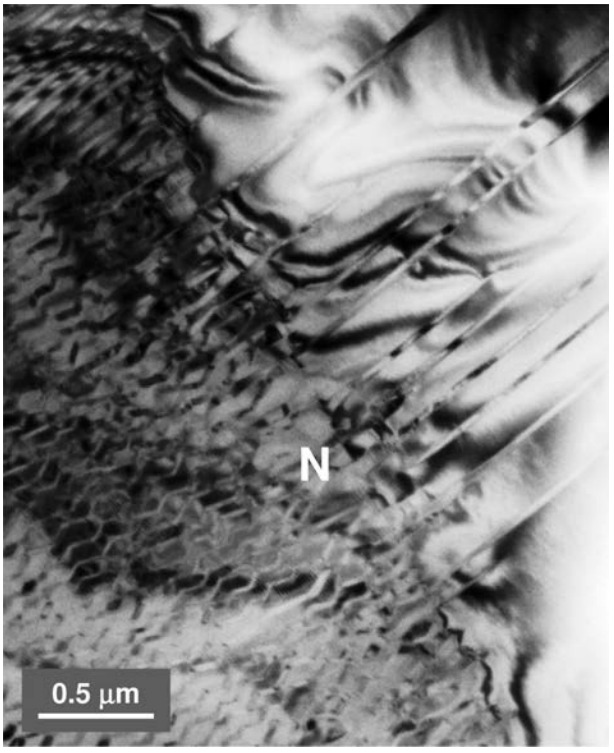

FIGURE 2. Bright-field TEM image from sample KS 41, viewed near the **a***b* plane, of a (010) boundary between braid cryptoperthite (left) and film microperthite (right) in an Or-rich patch. The lozenge-shaped areas in the braid microtexture are Albite-twinned albite, and the zigzag bands between them are low microcline in the "diagonal association" with interfaces in $\{\bar{6}\bar{6}1\}$ (see Brown et al. 1983 for detail). The film lamellae are low albite with Albite twinning at a fine scale, not visible in the image, in a matrix of tweed orthoclase (see Parsons et al. in prep., for detail). The film lamellae are in ~$(\bar{6}01)$ but appear not to be at right angles to (010) because the foil is not exactly parallel to **b**. They are semicoherent, with sub-regularly spaced misfit dislocation loops, enlarged to nanotunnels, not visible at this magnification. In places, such as to the right of N, film lamellae have nucleated on albite in braid, but in general they are independent of features in braid.

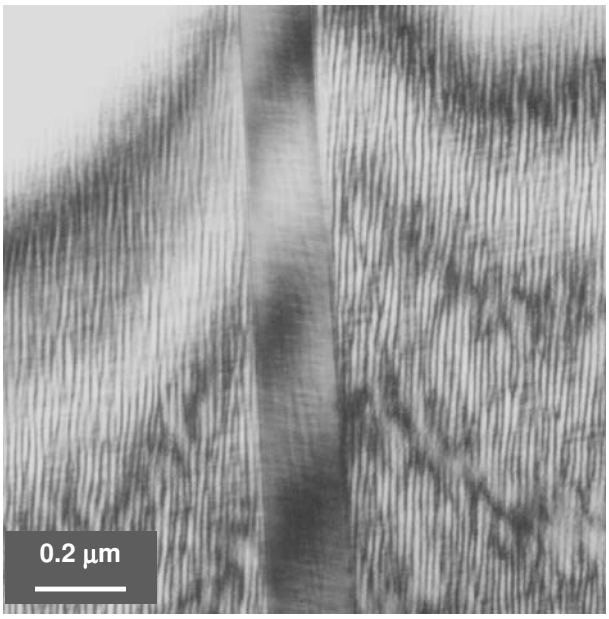

FIGURE 3. Dark-field TEM image of peristerite in sample KS 41, bulk composition $Ab_{92}An_7Or_1$, viewed from close to [001] using g = –130. The band slightly left of center is an Albite twin, bounded by (010). The strong, sinuous modulation (peristerite) in the outer twins makes an angle of ~8° with (010), corresponding with a plane close to (1,14,*l*). The central twin shows a tweed microstructure, but not the strong modulation in the adjacent twins. The tweed modulation nearly at 90° to (010) is visible in all three twins and in the central twin the second modulation is again 8° from (010).

The layered series is unusually and very strikingly layered (Parsons 1979; Parsons and Lee 2009). Sheets of dark-colored, "granular syenite" are separated by thicker, pale-colored layers of much coarser, "laminated syenite". Both syenite types are hypersolvus and the alkali feldspars have similar bulk compositions, in the range $Ab_{75}Or_{25}$ to $Ab_{45}Or_{55}$, with $<An_8$ (Brown et al. 1983). Parsons (1978) showed high turbidity in feldspars from the laminated syenite, whereas those in the granular syenites are usually glass-clear in section.

The granular syenite feldspars have regular, fully coherent, fine-scale (λ < 500 nm), "braid" crypto- and micro-perthitic microtextures (Fig. 1, right; Fig. 2, left), with morphologies controlled by coherency strain (Brown et al. 1983, 1997; Brown and Parsons 1984a, 1984b, 1988; Lee et al. 1997). The feldspars crystallized as homogeneous Na-sanidine at ~850 °C and exsolution began at ~700 °C (Fig. 4) initially in the form of straight lamellar mesocryptoperthites. In coherent braid cryptoperthites, diamond-shaped lozenges of low albite are enclosed in low microcline (Fig. 2).

The periodicity λ of the braid cryptoperthite in the granular syenites increases from ~40 nm at the top of the layered series to ~150 nm at the base (Brown et al. 1983) and $\log_{10}\lambda$ increases linearly with distance from the top of the layered series, indicating that the intrusion cooled predominantly through its roof. These λ are remarkably small, and similar, at the top, to those of volcanic rocks. Brown and Parsons (1984a) concluded that the small λ values resulted from the coupling of exsolution and framework ordering, but problems remain to which we return below.

The laminated syenite feldspars have much coarser (up to millimeter-scale), irregular patch microperthite intergrowths, replacing the braid cryptoperthite, which persists to variable extents within individual crystals (Fig. 1). The braid perthite shows the same relationship between stratigraphic position and λ as the granular syenites, but with larger values of λ. No firm explanation for this observation has been developed but cooling rate cannot have been the only factor controlling λ.

It is generally accepted that the development of turbid patch perthite in the laminated syenites, which Parsons and Brown (1984) called "deuteric coarsening", is the result of dissolution-reprecipitation reactions in a circulating aqueous fluid. The profound recrystallization accompanying these reactions was demonstrated using TEM by Worden et al. (1990), and the process treated in detail by Parsons and Lee (2009) and Parsons et

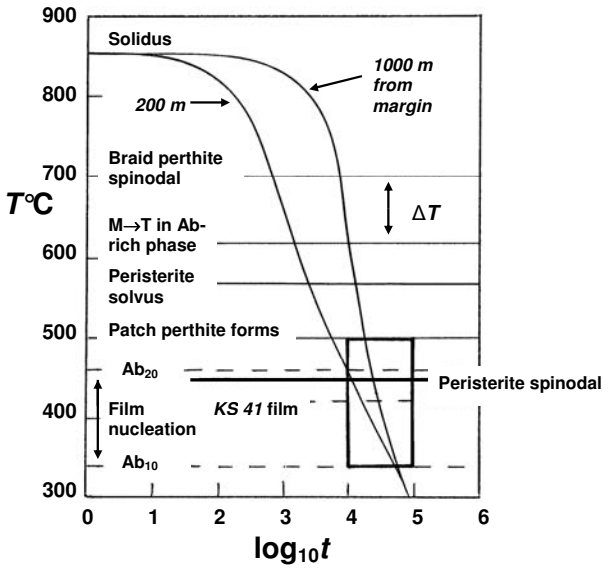

FIGURE 4. Cooling curves (t in yr) for the Klokken intrusion taken from Brown and Parsons (1984a, Fig. 10), for points 200 m and 1000 m in from the contact. The latter curve corresponds approximately to the position of sample KS 41. ΔT is the interval over which most of the coherent coarsening of braid cryptoperthite occurred (Brown and Parsons 1984a, Fig. 9). The vertical arrow at the bottom left indicates the range of T at which Or-rich patches within the range Ab_{20}-Ab_{10} encountered the coherent solvus of Yund (1974) for ordered feldspars, and a third broken line shows the equivalent T for sample KS 41 (Ab_{16}). Film perthite formation would begin at or slightly below these lines. The T at which the Ab-rich patches in sample KS 41 (An_8) would enter the peristerite conditional spinodal is inferred from Figure 2d in Carpenter (1981). The T of the peristerite solvus is taken from Carpenter (1994). Note that the dissolution-reprecipitation reaction leading to patch perthite formation occurred ~70 °C below this solvus (Parsons and Lee 2009) so that a metastable, homogeneous, relatively disordered plagioclase must have crystallized. The heavy box corresponds with box 2 in Figures 5a and 5b.

al. (2009a, 2009b). The reactions were essentially isochemical (Brown et al. 1983), and driven by reduction of elastic coherency strain energy in braid perthite, as proposed by Worden et al. (1990) and discussed theoretically by Brown and Parsons (1993). The braid microtexture is replaced by Ab- and Or-rich subgrains, which are often arranged in clusters. The deuteric reactions took place in the microcline stability field (the braid perthite intergrowths contain low microcline), the upper limit of which is usually placed at 500–480 °C (Fig. 4) (Brown and Parsons 1989; Kroll et al. 1991); this was confirmed using two-feldspar thermometry by Parsons et al. (2009a, 2009b).

DESCRIPTION OF FILM PERTHITE

Parsons and Lee (2009) reported film albite exsolution lamellae in Or-rich patches in laminated syenite feldspars (Figs. 1 and 2). The lamellae are semicoherent with periodicities of up to ~1 μm (their Figs. 6 and 7). Similar lamellae have been found in 12 out of 13 laminated syenite samples inspected using scanning electron microscopy (SEM) (Parsons et al. in prep.). In most laminated syenite samples, the matrix Or-rich feldspar is tartan twinned low microcline, but in KS 41, the subject of the present paper, it is orthoclase with tweed microstructure (Fig. 2). A possible explanation is that the locality of KS 41 is ~80 m from the margin of a sheet of syenodiorite that was emplaced under the roof of the intrusion after the layered series had solidified (Parsons 1979). It is possible that this heated and dehydrated KS 41 in the interval between patch perthite and film perthite formation. There are no other obvious microscale differences between the feldspars in KS 41 and other laminated syenites.

Electron probe microanalysis (EPMA) of an Or-rich patch in KS 41, using a 5 μm beam, gave a bulk composition of $Ab_{15.7}Or_{83.9}An_{0.3}$ (Parsons et al. in prep.). The albite films (Fig. 2) are very flat lenses in an irrational plane close to $(\bar{6}01)$, the plane of minimum strain energy appropriate for this composition (Willaime and Brown 1974). The morphology of coherent intergrowths in slowly cooled alkali feldspars is a function of bulk composition (Brown and Parsons 1988) and nearly straight lamellae are usual in this compositional range. Such extended lamellae must nucleate periodic misfit dislocations to accommodate strain (Waldron et al. 1994), and these occur on the KS 41 lamellae (see Parsons and Lee 2009, Fig. 7). TEM (Parsons et al. in prep.) shows that the sites of the dislocations have been enlarged by dissolution to produce networks of nanotunnels (Fitz Gerald et al. 2006). The lamellae are twinned at a fine scale (twin periodicity ≤40 nm) on the Albite law, and the twin periodicity varies with the thickness of the exsolution lamellae in the manner predicted by Willaime and Gandais (1972), showing that unless the twins are pseudotwins, Si-Al interdiffusion continued to <300 °C.

DESCRIPTION OF PERISTERITE

During TEM work to characterize the novel film microtextures we noticed that coexisting Ab-rich patches in KS 41 had a fine-scale, fully coherent lamellar microtexture with a mean λ of 17 nm, which we interpret to be a peristerite (Fig. 3). We have not, as yet, looked for peristerite in other Klokken intrusion samples. Peristerite intergrowths form in the bulk compositional range An_2-An_{17} and are intimate intergrowths of two plagioclase feldspars, $An_{1\pm1}$ and $An_{25\pm5}$, with different ordering patterns (Carpenter 1994). Exsolution is largely driven by the free energy of Si, Al ordering in albite. Because the ionic radii of Na^{1+} and Ca^{2+} are almost the same, there is no significant coherency strain. Brown (1989a) discusses the geometry of peristerite and Brown (1989b) and Carpenter (1994) discuss the kinetics of its formation. The usual orientation of lamellae is $(0\bar{8}1)$. It is generally agreed that the intergrowths begin to form at a "conditional spinodal", a spinodal curve that is contingent on Si-Al ordering (Carpenter 1981, 1994).

Because peristerite is usually sub-optical, descriptions are infrequent, and it is often regarded as a rarity. With one exception, all previous examples have been found in regional metamorphic rocks and pegmatites. Lee et al. (2003) studied detrital plagioclase feldspars in North Sea sedimentary rocks and found abundant peristerite grains, suggesting that peristerite is common in their metamorphic and possibly granitic, source-rocks. The only previous description of a possible peristerite within a perthite (Abart et al. 2009) is from a granulite facies rock. There, a lenticular microtexture was detected by elemental imaging with a high-resolution electron microprobe. It had an apparent

periodicity of about 1 μm and lamellar thicknesses of up to ~500 nm, although it is not stated whether the intergrowth is normal to the section surface and no crystallographic details are given. This intergrowth is coarser than any peristerite previously described (Brown 1989b) and its identity needs to be confirmed crystallographically.

The crystallographic detail of the KS 41 peristerite will be provided in Parsons et al. (in prep). It contains two modulations (Fig. 3). We did not observe even weak extra *b*, *c*, *d*, or *e* reflections in diffraction patterns (see Smith and Brown 1988, p. 12, for definitions). A strong, slightly sinuous lamellar microstructure, a few degrees from (010), in which both sets of lamellae bifurcate and correspondingly terminate, with wedge-shaped ends, suggests spinodal decomposition. There are much weaker "tweed" modulations, roughly at right angles, most easily seen in the Albite twin in the center of Figure 3. A similarly orientated tweed-scale modulation can be seen cutting the strong lamellar structure in the broader twins. Diffraction patterns show satellites on one set of twins only, corresponding with the strong peristerite structure. We do not know why the strong lamellae are confined to one set of twins. The relationship occurs elsewhere in KS 41, but is not universally seen. Lee et al. (2003, Fig. 4b) also illustrate variation in microstructure between adjacent twins, but the ultimate provenance of the detrital grains in their study is not known.

Nord et al. (1978) described similar microstructures in single, chemically zoned crystals from low-grade phyllites that reached peak metamorphism at ~350 °C. Janney and Wenk (1999) studied plagioclase from greenschist and amphibolite facies metamorphic rocks and found regions of strong lamellae but also other more complex microstructures including tweeds.

Coarsening kinetics

Film microperthite

Interdiffusion coefficients ($D_{Na\text{-}K}$) for Na and K in alkali feldspars have been determined in various ways including diffusion couple experiments (Christoffersen et al. 1983) and homogenization of natural perthitic feldspars (Brady and Yund 1983; Hokanson and Yund 1986). The latter workers studied the homogenization of two zigzag braid cryptoperthite intergrowths ($Ab_{66}Or_{32}An_2$ and $Ab_{60}Or_{35}An_5$) from the Klokken intrusion. They compared $D_{Na\text{-}K}$ values obtained in various studies and concluded that agreement was good and that the main variable was bulk crystal composition, which has a large effect on $D_{Na\text{-}K}$ as the solvus temperature is approached and the solid solution becomes more strongly non-ideal. $D_{Na\text{-}K}/X$ relationships at high *T*, and their variation with diffusion direction, are illustrated by Christoffersen et al. (1983, Figs. 2 and 3).

Yund et al. (1974) studied coarsening rates of lamellar cryptoperthite intergrowths directly by annealing a synthetic homogeneous ordered alkali feldspar, bulk $Ab_{67}Or_{33}$, made by ion-exchange. Using TEM they measured λ in the film cryptoperthite as it coarsened with time, *t*. The annealing method, using an initially homogeneous starting material, provides the most realistic way to approach the natural situation, particularly as it includes, ipso facto, the effect of coherency strain. Yund and Davidson (1978) carried out similar experiments using a disordered starting material at 560, 530, 500, and 470 °C for up to 1.5 yr (Fig. 5a, Box 1). The rate constant *k* (Eq. 1, below) was about twice that predicted by the Yund et al. (1974) study, in which Yund and Davidson (1978) suggested could be accounted for by the lack of absolute calibration of the micrographs used by Yund et al. (1974). Although the Klokken intrusion film perthite formed in an ordered framework, the Yund and Davidson (1978) experiments provide the most complete and reliable data from which to extrapolate to the natural examples. The largest value of λ produced experimentally was only 46 nm, such that extrapolation to our natural plutonic examples, in both *t* and λ, is extremely large. Yund and Chapple (1980) and Christoffersen and Schedl (1980) measured λ in alkali feldspars in a rhyolitic flow and dike and found reasonable agreement between λ calculated from Yund and Davidson's (1978) experiments and thermal histories from heat flow calculations. However, Snow and Yund (1985, 1988) found that in the Bishop Tuff, λ values were too large to be accounted for by any simple cooling history over the known age of the tuff, 0.7 Ma.

In most samples of film perthite in the Klokken intrusion, albite exsolution occurred in a microcline matrix. Patch perthite formation occurred after low microcline formation in braid, below 500–480 °C (the upper limit of microcline stability deduced by Kroll et al. 1991) and alkali exchange occurred between two fully ordered feldspar phases. Albite twins in albite have sometimes developed from Albite twins in adjacent microcline (Parsons et al. in prep.), suggesting that tartan Albite-Pericline twinning had developed before exsolution began. In sample KS 41, the matrix phase is tweed orthoclase (see above). Neither the present study nor experimental work (Smith and Brown 1988) suggests any systematic relationship between diffusivity of Na and K and framework order-disorder. However, coupling of simultaneous ordering and exsolution via coherency strains may have a very large effect on coarsening rates, discussed in connection with braid perthite below.

Brady (1987) proposed that diffusional exchange from the wedge-shaped ends of declining small lamellae to planar surfaces of adjacent, larger, growing lamellae was the main coarsening mechanism and showed that for spinodal decomposition, coarsening to a periodicity λ in time *t* is given by $\lambda^2 = \lambda_0^2 + kt$. The initial periodicity is λ_0, which Brady showed decreased with *T* and was <10 nm at 470 °C. It can be, therefore, ignored in the present case. By least-squares analysis of Yund and Davidson's data Brady obtained the Arrhenius relationship [*k* (m^2/s), activation energy E_a (J/mol), *T* Kelvin]:

$$k = (2.076 \times 10^{-14})\exp(-139\,825/RT). \quad (1)$$

The Klokken film perthite did not form by spinodal decomposition, but by coherent nucleation that, in places, is demonstrably heterogeneous (Fig. 2). Nevertheless, where lamellae are sub-regularly distributed and extend far from the margin of the Or-rich patch (as is the case for most lamellae in Fig. 2), and where we can be sure there are no intervening small lamellae and platelets (Parsons et al. in prep.), it is possible to estimate a diffusion distance, λ/2. The rate constant *k* in (Eq. 1) is functionally equivalent to *D* in the Einstein approximation $x^2 = Dt$ where *x* is the diffusion distance (m). We have used this relationship to

calculate the curves on Figure 5a, which shows the time taken, with respect to *T*, during isothermal annealing, for film perthite to coarsen to lamellar periodicities of 1 μm and 500 nm, which encompasses the range of the largest separations found in our TEM micrographs (Fig. 2 and Parsons et al. in prep).

Coherent exsolution of film perthite began at or just below the coherent solvus for ordered feldspars (Yund 1974). Ignoring their low An content, Or-rich patches in KS 41 ($Ab_{15.7}Or_{83.9}An_{0.3}$) would have intersected this curve at 420 °C. The cooling trajectory of the Klokken intrusion 1 km from its margin (Fig. 4), appropriate for the field location of KS 41, suggests that this will have occurred about 30 000 yr after crystallization. Figure 5a shows that film perthite annealed at 420 °C would have coarsened to λ of 500 nm after a further 3300 yr and to 1 μm in 13 000 yr. Models of spinodal decomposition (Abart et al. 2009), show that most coarsening occurs within 30 °C of the coherent spinodal. Because diffusion slows rapidly as *T* decreases this is also likely to be the case with exsolution following coherent nucleation. At 390 °C, the equivalent times are 9800 yr and 39 000 y. These times are all in good order-of-magnitude agreement with the cooling path in Figure 4.

Peristerite

Solvus and spinodal curves for peristerite are much less well known than the equivalent curves for perthite. The best estimate of the solvus is given by Carpenter (1994, Fig. 11) and Lee et al. (2003, Fig. 7). It is based on natural metamorphic assemblages analyzed by Spear (1980), Grove et al. (1983) and Ashworth and Evirgen (1985). For Ab-rich patches in KS 41 an average of 10 analytical TEM analyses with unfocused beams of diameter 150–200 nm gave a bulk composition of $Ab_{92.3}An_{6.4}Or_{1.3}$ and 26 EPMA analyses using a 5 or 10 μm beam gave $Ab_{90.9}An_{7.7}Or_{1.4}$. The solvus *T* for this composition is ~570 °C, ~70 °C above the *T* of patch perthite formation (Fig. 4). Because peristeritic exsolution is conditional on Si-Al ordering, we conclude that the Ab-rich patches grew inside the peristerite solvus with metastable disorder, as suggested by Nord et al. (1978) for peristerite intergrowths in low-grade phyllites. The likelihood of this growth mechanism is discussed by Carpenter and Putnis (1985) and Carpenter (1994).

The peristerite spinodal is even less well defined, but the bulk compositional range of natural peristerite intergrowths suggests that the An-rich limb is at ~An_{17} at low temperature. The approximate "conditional spinodal" of Carpenter (1981, Fig. 2d) suggests that spinodal decomposition would have begun at around ~450 °C in KS 41 (Fig. 4). Very fine-scale intergrowths would have formed rapidly and then coarsened to the observed λ of 17 nm. The modeling of Abart et al. (2009) suggests that coarsening would have been largely complete by around 420 °C.

Na-Ca inter-diffusion in plagioclase is considerably slower than Na-K interdiffusion in perthite, because charge-coupling requires NaSi-CaAl interdiffusion, and experimental work has been carried out at high *T*, well above the peristerite solvus, where diffusion is faster. There have been several studies in which $D_{NaSi\text{-}CaAl}$ has been obtained in homogenization experiments, reviewed by Smith and Brown (1988, Chap. 16), Brown (1989b) and Liu and Yund (1992). Unlike Na-K interdiffusion, NaSi-CaAl interdiffusion is strongly sensitive to the presence of water and the study of Liu and Yund (1992) was carried out with ~1 wt% water at 1500 MPa. Baschek and Johannes (1995) studied the homogenization of two peristerite samples at 1 GPa in the presence of a mixed N_2–H_2O fluid in the range $X_{H_2O} = 0$ to $X_{H_2O} = 0.5$, and showed that log *D* increased linearly by approximately two orders of magnitude over this range in X_{H_2O}. Analysis of fluids released by crushing a deuterically coarsened Klokken intrusion feldspar (Burgess et al. 1992) showed them to be largely aqueous, with 1.1 wt% Cl. We can be confident that peristerite and film perthite formation occurred in an essentially water-saturated environment, although at a much lower *P* than that used by Baschek and Johannes (1995), and by Liu and Yund (1992). We have used the latter work for our calculations (Fig. 5b), although the high *P* may have increased diffusion rate. The study of Baschek and Johannes (1995) is discussed further below.

The experiments of Liu and Yund (1992) were carried out in the range 1050–900 °C, for $t \leq 336$ h (Fig. 5b, Box 3). Their starting material was a peristerite from a pegmatite, $Ab_{91.9}An_{6.7}Or_{1.4}$ (similar to the peristerite in KS 41) with λ = 110 nm. Liu and Yund (1992) obtained:

$$D_{NaSi\text{-}CaAl} = (3 \times 10^{-8})\exp(-303\,000/RT) \quad (2)$$

(where *D* and the pre-exponential term, *A*, are m^2/s, and the activation energy, E_a, is J/mol) which we have used to calculate curve A on Figure 5b. This gives coarsening times of 520 000 yr at 450 °C and 4 606 000 yr at 420 °C, much longer than the times calculated for the film perthite, and incompatible with the cooling trajectory for the Klokken intrusion (Figs. 4 and 5, Box 2).

We have taken two different approaches for analyzing this difference:

(1) Other studies of the thermal history of peristerite intergrowths (Nord et al. 1978; Brown 1989b; and review of Carpenter 1994) have led to the conclusion that homogenization experiments at high *T* underestimate peristerite coarsening rates at solvus temperature. Brown (1989b) discusses possible reasons for these discrepancies, including the role of hydrogen (structural protons), which are known to increase rates of framework ordering, as is high pressure. The high-*P*, water-containing experiments of Liu and Yund (1992) might be expected to lead to enhanced diffusion rates, but without our suggested modification these nevertheless still appear too slow to explain the Klokken sample peristerite intergrowths. We calculate (Fig. 5, curve B) that a modest 10% reduction in activation energy, E_a, to 270 000 J/mol, gives 2150 yr at 450 °C and 15 000 yr at 420 °C, bringing these times into the same range as the film perthite coarsening times. However, curve B does not match the experimental observations of Liu and Yund (1992) (Fig. 5, Box 3).

(2) Change in both *A* and E_a allows a better linkage of the Liu and Yund (1992) observations to the inferred peristerite coarsening times. A choice for E_a of 220 000 J/mol and *A* of 9×10^{-12} m^2/s produces a path in log *t*-*T* space (Fig. 5, curve C) that gives fair agreement with both experimental and natural constraints. Carpenter's (1981) estimate of the position of the conditional spinodal (450 °C for An_8) was necessarily very rough, but any value in the range 475–425 °C would lead to completion of coarsening within box 2 on Figure 5. Note that this pair of E_a and *A* values, recalculated to compare with peristerite-homogenization

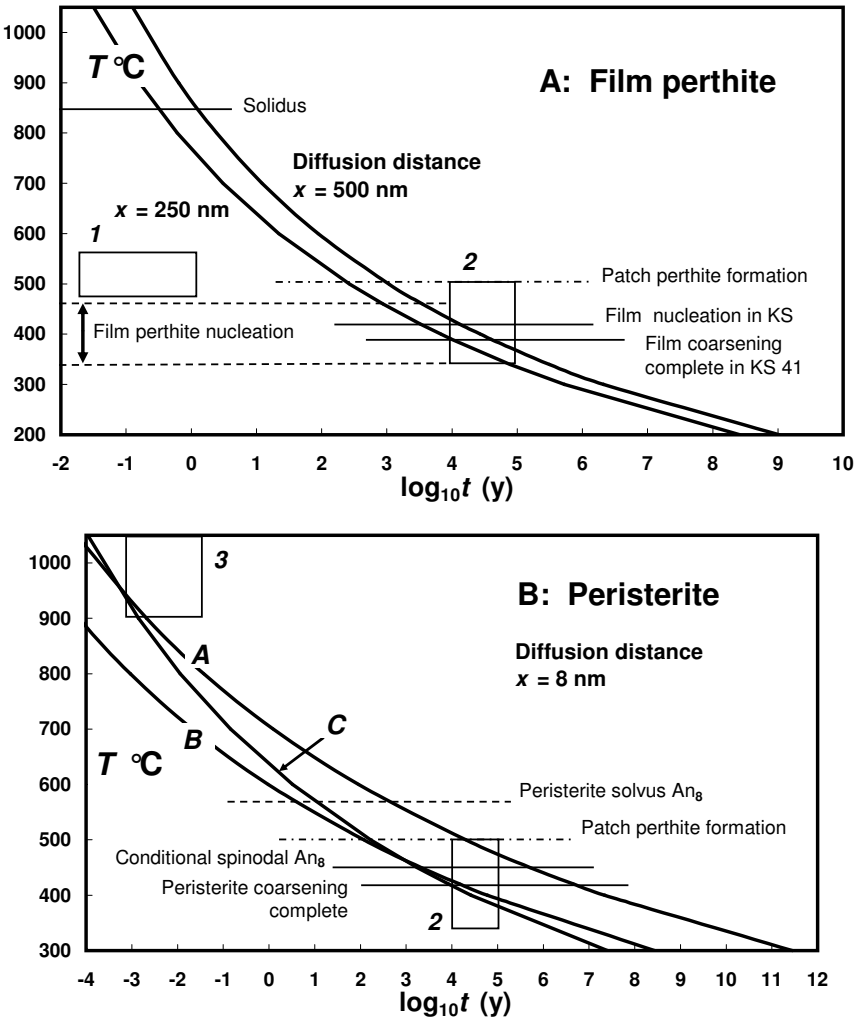

FIGURE 5. Curves showing isothermal annealing times required to reach observed lamellar periodicities λ in film perthite and peristerite coexisting in patch perthite in sample KS 41. Sources for the various horizontal lines are given in Figure 4. We have suggested that coarsening was essentially complete 30 °C below the beginning of exsolution, following Abart et al. (2009). Box 2 corresponds with the box on the Klokken intrusion cooling trajectory shown on Figure 4. (**a**) Film perthite with λ of 1 and 0.5 μm using the experimental data of Yund and Davidson (1978), calculated from present Equation 1. $\lambda = 2x$, the diffusion distance. Box 1 indicates the *T/t* range of the Yund-Davidson experiments, emphasizing the very long extrapolation to the natural situation. (**b**) Peristerite with λ of 16 nm. The *T/t* range of Liu and Yund's (1992) homogenization experiments is indicated by box 3. Curve A uses the values of Liu and Yund (1992) of E_a (303 000 J/mol) and A (3×10^{-8} m^2/s). Curve B uses an E_a of 270 000 J/mol, and curve C uses an E_a 220 000 J/mol and A 9×10^{-12} m^2/s. Curve C passes through both the experimental data and the box representing the Klokken intrusion cooling history. It is also within the error limits in log D for results at all four experimental temperatures investigated by Liu and Yund (1992).

observations in Liu and Yund (1992, their Fig. 4, showing log D against $1/T$) clearly produces an inferior fit, but one that falls within the uncertainty limits (±0.3 log units in D) estimated by Liu and Yund (1992) to apply across the range of T that they examined. However, the implied value for E_a (and possibly for A) represents a major shift from the values preferred by Liu and Yund (1992), and possibly, unreasonably so.

The coarsest peristerite intergrowths investigated using TEM and reported in the literature have λ up to 300 nm (x = 150 nm) (Smith and Brown 1988) and very rarely they are coarse enough to be visible optically (Smith and Brown 1988, Fig. 19.28). The intergrowth imaged using a high-resolution electron microprobe by Abart et al. (2009) has λ of ~1 μm but crystallographic details are not given. Table 1 shows coarsening times to these dimensions for the combinations of A and E_a used to calculate curves A and C on Figure 5b. The new values can lead to intergrowths in geologically feasible times for regional metamorphism at both scales, whereas the Liu and Yund (1992) parameterization requires unfeasibly long annealing times even for the 300 nm intergrowths. Peristerite described by Nord et al. (1978), with λ of 12 nm, occurs in phyllites that experienced peak metamorphism at only 350 °C. Again, curve C on Figure 5b suggests that this λ can be reached over geologically reasonable time scales.

From their experiments using mixed $H_2O - N_2$ fluids Baschek

and Johannes (1995) suggested that the T dependence of the diffusion coefficient for $X_{H_2O} = 0.5$ could be described by:

$$D_{NaSi-CaAl} = 17\exp(-465\,000/RT). \quad (3)$$

This expression leads to t for coarsening of the Klokken sample peristerite, over a diffusion distance of 8 nm (Fig. 5b), on the order of 10^9 yr at the peristerite spinodal and 10^{10} yr for completion of coarsening. These impossibly long coarsening times primarily arise from the effect of low X_{H_2O} on log D, and to a lesser extent on a correction applied by Baschek and Johannes (1995) to the apparent homogenization times observed using TEM. Because annealing T and t possible in the Klokken intrusion are relatively well defined (Fig. 5b, Box 2) the present study and the Baschek and Johannes (1995) work illustrate clearly the role of aqueous fluids in peristerite diffusion kinetics.

The presence of peristerite in the small, high-level Klokken syenite intrusion implies that it should be commonplace in Ab-rich plagioclase in many granitoid intrusions. Or-rich alkali feldspars in granites have similar bulk compositions to the Or-rich patches in Klokken intrusion feldspars and nearly always contain film microperthite on similar or coarser scales (e.g., Waldron et al. 1994; Lee et al. 1995). The abundance of peristerite in detrital plagioclase in North Sea reservoir rocks (Lee et al. 2003) also suggests that peristerite is considerably more abundant than usually presumed.

Braid perthite

Brown et al. (1983) pointed out that the periodicity of the braid cryptoperthite intergrowths in the Klokken intrusion is extremely small, measured λ ranging from ~40 nm at the top of the layered series to ~400 nm at the base. The smallest λ are similar to volcanic rocks and are less than the lamellar spacing (46 nm) produced after experimental annealing for 1.5 yr at 560 °C by Yund and Davidson (1978). These small λ are not unique to Klokken; similar values were later found in feldspars in the very much larger (~20 km diameter) but compositionally similar Coldwell syenite (Waldron and Parsons 1992). Coldwell intrusion feldspars have microtextures similar to those in the Klokken intrusion. Within ≤500 m of the outer contact they have straight lamellae with λ of ~50 nm. These give way inward, via a zone of wavy cryptoperthite, to braid perthite with slightly larger λ of ~80 nm, in the interior.

TABLE 1. Calculated annealing times (m.y.) to produce coarse peristerite intergrowths

	Liu and Yund (1992)	This study
A (m²/s)	3×10^{-8}	9×10^{-12}
E_a (J/mol)	303 000	220 000
T (°C)	t (m.y.)	
λ/2 = 150 nm*		
500	7.03	0.058
450	183	0.616
400	>	9.337
300	>	>
λ/2 = 500 nm†		
500	78.1	0.643
450	2032	6.849
400	>	103.7
300	>	>

Note: > age of the Earth.
* Largest periodicity listed by Smith and Brown (1988).
† Microtexture imaged by Abart et al. (2009) using a high-resolution electron microprobe.

These small periodicities remain puzzling, more so in the light of our discovery in the Klokken intrusion of coexisting film perthite with considerably larger λ, despite its much lower exsolution temperature. Brown and Parsons (1984a) concluded that "some mechanism must exist which slows or largely prevents primary coarsening in slowly cooled plutons", but this statement is evidently too general. The film perthite in Or-rich patches, formed by deuteric coarsening below 500 °C, coexisting with residual braid perthite, has coarsened to a periodicity that, as we show above, is in good agreement with the calculated cooling history of the pluton. Furthermore, film perthite, very similar to that in the Klokken intrusion, is common in alkali feldspars from granitoids, which have bulk compositions in the same range as those in the Klokken intrusion Or-rich patches. In the Shap granite (Lee et al. 1995), a pluton of comparable size to the Klokken intrusion, film periodicities are similar, whereas in the larger Okueyama pluton (Yuguchi and Nishiyama 2007) periodicities are larger, increasing from ~5 μm near the roof to ~15 μm 800 m below. In general terms these film perthite intergrowths conform to extrapolations of the Yund and Davidson (1978) coarsening experiments.

Brown and Parsons (1984a) conjectured that, in the Klokken intrusion, coarsening took place rapidly after the feldspars intersected the coherent spinodal (Fig. 4), which is coincident with the coherent solvus near its critical T (~670 °C for An-free feldspars) and critical composition (near $Ab_{60}Or_{40}$). Initially, the coexisting phases were both monoclinic (this two-sanidine stage is labeled ΔT on Fig. 4) and film perthite formed in a plane near $(\bar{6}01)$. At ~600 °C, the Ab-rich phase intersected the monoclinic-triclinic shearing transformation (Fig. 4, M→T) and long-period Albite twins developed to reduce strain energy. As the framework ordered, these became true ordered and anti-ordered twins, the obliquity of the twins increased, and their periodicity decreased. In braid perthite, Albite twin periodicities depend on the mean periodicity of the braid intergrowth, not on the local thickness within the lozenge-section albite columns (Fig. 2 and see many illustrations in Brown and Parsons 1984a). Formation of braid took place during further cooling by rotation of lamellar interfaces from $(\bar{6}01)$ to $\{\bar{6}\,\bar{6}1\}$ to minimize strain. Precursor straight lamellae are not preserved in the Klokken intrusion, but examples were found later in the Coldwell syenites (Waldron and Parsons 1992) where all stages in the progression to braid texture can be followed. Brown and Parsons (1984a) concluded that primary coarsening stops in braid perthite intergrowths when exsolution lamellae are straight because Si-Al interdiffusion is required to change the left-right ordering pattern of adjacent twins.

In contrast, in the low-T film perthite intergrowths described here, the periodicity of Albite twins is a function of local lamellar width, to minimize strain energy (Willaime and Gandais 1972). Exsolution of film lamellae occurs when the framework has a high degree of order, and the process is not coupled to changing order and symmetry in the framework. Film lamellae are able to coarsen more than braid, although coarsening is occurring at considerably lower temperature (Fig. 4).

Whereas it seems very likely that coupling between Na-K and Si-Al interdiffusion through coherency strains underlies

the very small periodicities in the braid feldspars, one serious problem, pointed out by Brown and Parsons (1984a) remains. The time taken to pass through the ΔT interval (Fig. 4), when both phases are monoclinic, on any feasible cooling trajectory, is much longer than the time taken to produce similar periodicities in the laboratory. Figure 4 implies ~700 yr 200 m from the intrusion margin, and ~2000 yr 1000 m in. Equation 1 predicts that the primary periodicities of braid perthite, which are in the range 40 to 400 nm, would be reached in, respectively, 0.034 yr and 3.4 yr at the coherent spinodal (~670 °C), and 0.142 yr and 14.2 yr at the M→T transition (~600 °C). One possible explanation is that the M→T transition intersects the coherent solvus close to its critical T, so that ΔT is very small. The line for the transition shown by Brown and Parsons (1984a, their Fig. 9) is very poorly constrained. Another possibility is that the small An content of the bulk crystals slows coarsening because of Na-Si and Ca-Al coupling. In both the Klokken and Coldwell intrusions, the smallest λ occur in the most An-rich crystals (An_3 in Klokken, An_4 in the Coldwell intrusion), but overall there is no clear coupling between An and periodicity. Furthermore, An would increase exsolution T, possibly compensating for its effect on coarsening rate.

Concluding remarks

Despite the very long extrapolation in t and lamellar periodicity, coarsening kinetics of film perthite, calculated from laboratory exsolution studies (Yund and Davidson 1978), lead to coarsening time scales in good order-of-magnitude agreement with the calculated cooling history of the Klokken intrusion, implying times in the range 3 to 39 ky. For the peristerite intergrowth, extrapolation of interdiffusion coefficients obtained by homogenization of a natural peristerite (Liu and Yund 1992) leads to an Arrhenius relationship that implies excessively long annealing times for the Klokken intrusion occurrence. Peristerite coarsening can be accommodated with the film perthite thermal history by changes to the constants describing rates of NaSi-CaAl interdiffusion.

We find that the relationship:

$$D_{\text{NaSi-CaAl}} = (9 \times 10^{-12})\exp(-220\,000/RT)$$

(where D and the pre-exponential term, A, are m^2/s, and the activation energy, E_a, is J/mol) leads to coarsening rates compatible with the experimental data of Liu and Yund (1992), the cooling path of the Klokken intrusion, and the coarsening rate of the coexisting film perthite. An equivalent expression obtained by Baschek and Johannes (1995) for a fluid with X_{H_2O} of 0.5 leads to coarsening times many orders of magnitude too long for the Klokken intrusion, confirming the role of H_2O in the fluid phase in peristerite coarsening.

Acknowledgments

This work was partially funded by the NERC under research grant NER/A/S/2001/01099 to Ian Parsons. He is grateful to the Royal Societies of London and Edinburgh for support for travel to Australia.

References cited

Abart, R., Petrishcheva, E., Wirth, R., and Rhede, D. (2009) Exsolution by spinodal decomposition II: perthite formation during slow cooling of anatexites from Ngoronghoro, Tanzania. American Journal of Science, 309, 450–475.

Ashworth, J.R. and Evirgen, M.M. (1985) Plagioclase relations in pelites, central Menderes Massif, Turkey. I. The peristerite gap with coexisting kyanite. Journal of Metamorphic Geology, 3, 207–218.

Baschek, G. and Johannes, W. (1995) The estimation of NaSi-CaAl interdiffusion rates in peristerite by homogenization experiments. European Journal of Mineralogy, 7, 295–307.

Brady, J.B. (1987) Coarsening of fine-scale exsolution lamellae. American Mineralogist, 72, 697–706.

Brady, J.B. and Yund, R.A. (1983) Interdiffusion of K and Na in alkali feldspars: homogenization experiments. American Mineralogist, 68, 106–111.

Brown, W.L. (1989a) Glide twinning and pseudotwinning in peristerite: twin morphology and propagation. Contributions to Mineralogy and Petrology, 102, 306–312.

——— (1989b) Glide twinning and pseudotwinning in peristerite: Si, Al diffusional stabilization and implications for the peristerite solvus. Contributions to Mineralogy and Petrology, 102, 313–320.

Brown, W.L. and Parsons, I. (1984a) Exsolution and coarsening mechanisms and kinetics in an ordered cryptoperthite series. Contributions to Mineralogy and Petrology, 86, 3–18.

——— (1984b) The nature of potassium feldspar, exsolution microtextures and development of dislocations as a function of composition in perthitic alkali feldspars. Contributions to Mineralogy and Petrology, 86, 335–341.

——— (1988) Zoned ternary feldspars in the Klokken intrusion: exsolution textures and mechanisms. Contributions to Mineralogy and Petrology, 98, 444–454.

——— (1989) Alkali feldspars: ordering rates, phase transformations and behaviour diagrams for igneous rocks. Mineralogical Magazine, 53, 25–42.

——— (1993) Storage and release of elastic strain energy: the driving force for low temperature reactivity and alteration of alkali feldspars. In J.N. Boland and J.D. Fitz Gerald, Eds., Defects and Processes in the Solid State: Geoscience Applications. The McLaren Volume (Developments in Petrology 14). Elsevier, Amsterdam, 267–290.

Brown, W.L., Becker, S.M., and Parsons, I. (1983) Cryptoperthites and cooling rate in a layered syenite pluton: a chemical and TEM study. Contributions to Mineralogy and Petrology, 82, 13–25.

Brown, W.L., Lee, M.R., Waldron, K.A., and Parsons, I. (1997) Strain-driven disordering of low microcline to low sanidine during partial phase separation in microperthites. Contributions to Mineralogy and Petrology, 127, 304–313.

Burgess, R., Kelley, S.P., Parsons, I., Walker, F.D.L., and Worden, R.H. (1992) ^{40}Ar-^{39}Ar analysis of perthite microtextures and fluid inclusions in alkali feldspars from the Klokken syenite, South Greenland. Earth and Planetary Science Letters, 109, 147–167.

Carpenter, M.A. (1981) A 'conditional spinodal' within the peristerite miscibility gap of plagioclase feldspars. American Mineralogist, 66, 553–560.

——— (1994) Subsolidus phase relations of the plagioclase feldspar solid solution. In I. Parsons, Ed., Feldspars and their reactions, p. 221–269. Kluwer, Dordrecht.

Carpenter, M.A. and Putnis, A. (1985) Cation order and disorder during crystal growth: some implications for natural mineral assemblages. In A.B. Thompson, D.C. Rubie, Eds., Metamorphic reactions. Advances in Physical Geochemistry, 4, 1–26. Springer, Berlin.

Christoffersen, R. and Schedl, A. (1980) Microstructure and thermal history of cryptoperthites in a dike from Big Bend, Texas. American Mineralogist, 65, 444–448.

Christoffersen, R., Yund, R.A., and Tullis, J. (1983) Inter-diffusion of K and Na in alkali feldspars: diffusion couple experiments. American Mineralogist, 68, 1126–1133.

Fitz Gerald, J.D., Parsons, I., and Cayzer, N. (2006) Nanotunnels and pull-aparts: Defects of exsolution lamellae in alkali feldspars. American Mineralogist, 91, 772–783.

Grove, T.L., Ferry, J.M., and Spear, F.S. (1983) Phase transitions and decomposition relations in calcic plagioclase. American Mineralogist, 68, 41–59.

Harper, C.L. (1988) On the nature of time in cosmological perspective. Ph.D. thesis, University of Oxford, U.K.

Hokanson, S.A. and Yund, R.A. (1986) Comparison of alkali interdiffusion rates for cryptoperthites. American Mineralogist, 71, 1409–1414.

Jaeger, J.C. (1968) Cooling and solidification of igneous rocks. In H.H. Hess and A. Poldervaart, Eds., Basalts, 503–536. Wiley, New York.

Janney, D.E., and Wenk, H.-R. (1999) Peristerite exsolution in metamorphic plagioclase from the Lepontine Alps: An analytical and transmission electron microscope study. American Mineralogist, 84, 517–527.

Kroll, H., Krause, C., and Voll, G. (1991) Disordering, reordering and unmixing in alkali feldspars from contact-metamorphosed quartzites of the Ballachulish aureole, N.W. Scotland. In G. Voll, J. Töpel, and F. Seifert, Eds., Equilibrium and kinetics in contact metamorphism. The Ballachulish igneous complex and its aureole. Springer, Heidelberg, 267–296.

Lee, M.R., Waldron, K.A., and Parsons, I. (1995) Exsolution and alteration microtextures in alkali feldspar phenocrysts from the Shap granite. Mineralogical Magazine, 58, 63–78.

Lee, M.R., Waldron, K.A., Parsons, I., and Brown, W.L. (1997) Feldspar–fluid

interactions in braid microperthites: pleated rims and vein microperthites. Contributions to Mineralogy and Petrology, 127, 291–304.
Lee, M.R., Thompson, P., Poeml, P., and Parsons, I. (2003) Peristeritic plagioclase in North Sea hydrocarbon reservoir rocks: implications for diagenesis, provenance and stratigraphic correlation. American Mineralogist, 88, 866–875.
Liu, M. and Yund, R.A. (1992) NaSi-CaAl interdiffusion in plagioclase. American Mineralogist, 77, 275–283.
Nord, G.L., Hammarstrom, J., and Zen, E-an (1978) Zoned plagioclase and peristerite formation in phyllites from southwestern Massachusetts. American Mineralogist, 63, 947–955.
Parsons, I. (1978) Feldspars and fluids in cooling plutons. Mineralogical Magazine, 42, 1–17.
——— (1979) The Klokken gabbro–syenite complex, South Greenland: Cryptic variation and origin of inversely graded layering. Journal of Petrology, 20, 653–694.
——— (1981) The Klokken gabbro–syenite complex, South Greenland: Quantitative interpretation of mineral chemistry. Journal of Petrology, 22, 233–260.
Parsons, I. and Brown, W.L. (1984) Feldspars and the thermal history of igneous rocks. In W.L. Brown, Ed., Feldspars and feldspathoids. Structures, properties and occurrences. Reidel, Dordrecht, 317–371.
Parsons, I. and Lee, M.R. (2009) Mutual replacement reactions in alkali feldspars I: microtextures and mechanisms. Contributions to Mineralogy and Petrology, 157, 641–661.
Parsons, I., Rex, D.C., Guise, P., and Halliday, A.N. (1988) Argon loss by alkali feldspars. Geochimica et Cosmochimica Acta, 52, 1097–1112.
Parsons, I., Magee, C., Allen, C., Shelley, M.J., Lee, M.R. (2009a) Mutual replacement reactions in alkali feldspars II: trace element partitioning and geothermometry. Contributions to Mineralogy and Petrology, 157, 663–687.
——— (2009b) Erratum. Mutual replacement reactions in alkali feldspars II: trace element partitioning and geothermometry. Contributions to Mineralogy and Petrology, 157, 689–690.
Smith, J.V. and Brown, W.L. (1988) Feldspar Minerals, second edition, volume 1. Springer Verlag, Berlin, pp. 828.
Snow, E. and Yund, R.A. (1985) Thermal history of a Bishop Tuff section as determined from the width of cryptoperthite lamellae. Geology, 13, 50–53.
——— (1988) Origin of cryptoperthites in the Bishop Tuff and their bearing in its thermal history. Journal of Geophysical Research, 93, 8975–8984.
Spear, F.S. (1980) NaSi–CaAl exchange equilibrium between plagioclase and amphibole. Contributions to Mineralogy and Petrology, 72, 33–41.
Waldron, K.A. and Parsons, I. (1992) Feldspar microtextures and the multistage thermal history of syenites from the Coldwell Complex, Ontario. Contributions to Mineralogy and Petrology, 111, 222–234.
Waldron, K.A., Lee, M.R., and Parsons, I. (1994) The microstructures of perthitic alkali feldspars revealed by hydrofluoric acid etching. Contributions to Mineralogy and Petrology, 116, 360–364.
Willaime, C. and Gandais, M. (1972) Study of exsolution in alkali feldspars. Calculation of elastic stresses inducing periodic twins. Physica Status Solidi, 9, 529–539.
Willaime, C. and Brown, W.L. (1974) A coherent elastic model for the determination of the orientation of exsolution boundaries: application to the feldspars. Acta Crystallographica, A30, 316–331.
Worden, R.H., Walker, F.D.L., Parsons, I., and Brown, W.L. (1990) Development of microporosity, diffusion channels and deuteric coarsening in perthitic alkali feldspars. Contributions to Mineralogy and Petrology, 104, 507–515.
Yuguchi, T. and Nishiyama, T. (2007) Cooling process of a granitic body deduced from the extents of exsolution and deuteric sub-solidus reactions: Case study of the Okueyama granitic body, Kyushu, Japan. Lithos, 97, 395–421.
Yund, R.A. (1974) Coherent exsolution in the alkali feldspars. In A.W. Hofmann, B.J. Giletti, H.S. Yoder Jr., R.A. Yund, Eds., Geochemical Transport and Kinetics. Carnegie Institution of Washington Publication 634, 173–184.
Yund, R.A. and Chapple, W.M. (1980) Thermal histories of two lava flows estimated from cryptoperthite lamellar spacings. American Mineralogist, 65, 438–443.
Yund, R.A. and Davidson, P. (1978) Kinetics of lamellar coarsening in cryptoperthites. American Mineralogist, 63, 470–477.
Yund, R.A., McLaren, A.C., and Hobbs, B.E. (1974) Coarsening kinetics of the exsolution microstructure in alkali feldspar. Contributions to Mineralogy and Petrology, 48, 45–55.

Manuscript received December 22, 2010
Manuscript accepted June 14, 2011
Manuscript handled by Daniel Harlov